

Development of a Time-Domain Simulation Tool for Offshore Wind Farms

Hyungyu Kim^{*}, Kwansoo Kim^{*}, Insu Paek[†], and Neungsoo Yoo^{**}

^{*}Department of Convergence System Engineering, Kangwon National University, Chuncheon, Korea

^{†**}Department of Mechanical and Mechatronics Engineering, Kangwon National University, Chuncheon, Korea

Abstract

A time-domain simulation tool to predict the dynamic power output of wind turbines in an offshore wind farm was developed in this study. A wind turbine model consisting of first or second order transfer functions of various wind turbine elements was combined with the Ainslie's eddy viscosity wake model to construct the simulation tool. The wind turbine model also includes an aerodynamic model that is a look up table of power and thrust coefficients with respect to the tip speed ratio and pitch angle of the wind turbine obtained by a commercial multi-body dynamics simulation tool. The wake model includes algorithms of superposition of multiple wakes and propagation based on Taylor's frozen turbulence assumption. Torque and pitch control algorithms were implemented in the simulation tool to perform max-C_p and power regulation control of the wind turbines. The simulation tool calculates wind speeds in the two-dimensional domain of the wind farm at the hub height of the wind turbines and yields power outputs from individual wind turbines. The NREL 5MW reference wind turbine was targeted as a wind turbine to obtain parameters for the simulation. To validate the simulation tool, a Danish offshore wind farm with 80 wind turbines was modelled and used to predict the power from the wind farm. A comparison of the prediction with the measured values available in literature showed that the results from the simulation program were fairly close to the measured results in literature except when the wind turbines are congruent with the wind direction.

Key words: Eddy Viscosity, Numerical Wake Model, Wake, Wind Farm

I. INTRODUCTION

As wind power plants become larger in size, the importance of fatigue loading as well as power production from wind turbines is increasing. Offshore wind power plants have gained worldwide attention because of the advantages in wind turbine capacity, farm size, and wind energy, compared to onshore wind turbines. However, the cost of energy (COE) of offshore wind farms is significantly higher than their onshore counterparts, thus many researches have been conducted to reduce the COE of offshore wind farms such as the optimal placement of wind turbines, monitoring and prediction of parts failure, and wind farm control and benefit in annual power production and load,

operation, and maintenance [1]-[6]. Among these research topics, using wind farm control algorithm is advantageous because it can be implemented in existing wind farms without modifying the wind turbine and farm layout. However, before implementing the wind farm control algorithm to a wind farm, it is essential to verify the algorithm using various means such as simulations and experiments. A simulation tool that can simulate a wind turbine's dynamic power output in a wake field of the wind farm in the time domain can be considered.

The objective of this study was to develop a simple and approximate time-domain simulation tool to simulate the dynamic power outputs of wind turbines in an offshore wind farm and be used to validate a wind farm control algorithm in the future. Although several commercial wind farm simulation tools exist, they are based on the Weibull representation of the wind field and power curve of a wind turbine. These tools can be used to estimate the annual energy production of a wind farm but not for dynamic wind farm simulation and validation of wind farm algorithms [7]-[10].

A number of similar investigations focused on the

Manuscript received Dec. 30, 2014; accepted Mar. 4, 2015

Recommended for publication by Associate Editor Il-Yop Chung.

[†]Corresponding Author: paek@kangwon.ac.kr

Tel: +82-2-251-6371, Fax: +82-2-259-5551, Kangwon Nat'l University

^{*}Dept. of Convergence System Eng., Kangwon Nat'l Univ., Korea

^{**}Dept. of Mechanical & Mechatronics Eng., Kangwon Nat'l Univ., Korea

time-domain simulation of a wind farm [11], [12]. A CFD solver for the incompressible Navier-Stokes equation coupled with FAST, an open source wind turbine simulator based on multi-body dynamics, was used for a wind farm simulation [11]. However, it required significant computational power and is not suitable for fast wind farm simulation. A wind farm simulation tool requiring less computational power was developed, however the simple engineering wake model based on mass conservation in a linearly-expanding wake field was used, and the superposition of multiple wakes was not considered [12]. The simulation tool is developed using MATLAB with a combination of m-scripts and Simulink, thus not suitable for fast simulation of a wind farm with tens and hundreds of wind turbines.

In this study, a wind farm simulation tool that requires low computational power for a fast simulation for a wind farm with hundreds of wind turbines; the simulation tool is not coupled with a simple engineering wake model, rather, a more accurate model was developed. To develop this model, a C code consisting of a wake model was developed based on the eddy viscosity turbulence closure, wake propagation algorithm, wake superposition algorithm, and NREL 5 MW wind turbine model. The developed time domain wind farm simulation tool was validated with the experimental results from an offshore wind farm in Europe available in literature.

II. TIME DOMAIN WIND FARM SIMULATION

A. Wind Field Generation

To simulate the ambient wind field, turbulence must be produced. The ambient turbulence applies mechanical loads on the wind turbines and causes fluctuations in the electrical power generation of the wind turbines. The turbulent wind field can be expressed as a summation of the average wind speed and turbulence, and the turbulence can be obtained from spectrum models such as von Karman [13] and Kaimal spectrums. In this study, Kaimal spectrum that was used for the turbulence is known to correspond with the Kolmogorov theory, and it is also recommended by the standard, IEC 61400-1[14].

Originally, the ambient wind is represented by a three-dimensional wind field including wind shear in the vertical direction and turbulence in the downstream direction. However, a three-dimensional wind field propagation requires significant computer resources, and it is not suitable to simulate a large offshore wind farm having tens or hundreds of wind turbines. In this study, a two-dimensional wind field covering the lateral and downstream directions at the hub height of the wind turbines was generated by the commercial program using DNV·GL Bladed.

Fig. 1 shows the turbulent wind data generated by DNV·GL Bladed at the hub height, as well as the average rotor wind data. The average wind speed and turbulence intensity are

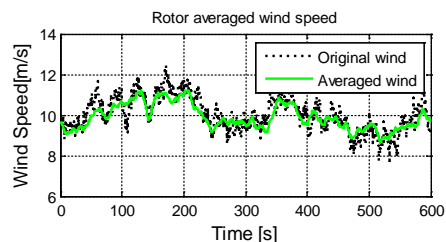


Fig. 1. Time variant wind speed at the rotor center of the wind turbine and rotor averaged wind speed.

10m/s and 0.09, respectively. The dotted line with many high frequency components shows the wind speed at the hub center of the wind turbine, whereas the solid line with a relatively weak fluctuation component shows the average rotor wind speed.

B. Wake Model

To exemplify the wake from a single wind turbine, the eddy viscosity wake model proposed by Ainslie [15] was used. The mathematical expression of the model is shown in Equation (1). The model is based on Reynolds-averaged Navier-Stokes equation (RANS) and assumes an axi-symmetric flow field. The model disregards the pressure gradient in the downstream direction that dominates the wind field near the field wake region; the area is known have a distance that is twice the rotor diameter from the upstream wind turbine. Hence the model is not suitable to predict the near-field wake. A rotor with a diameter of approximately six to twelve is used for turbine spacing in offshore wind farms; disregarding the downstream pressure gradient in the model was acceptable. The Ainslie model or any of its variations is applied in a few commercial codes that are commonly used for wind turbine analysis and wind farm design and analysis. Equation (1) shows the governing equation of the Ainslie's eddy-viscosity wake model.

$$U \frac{\partial U}{\partial x} + V \frac{\partial U}{\partial r} = -\frac{1}{r} \left(\frac{\partial \overline{u'v'}}{\partial r} \right), \quad -\overline{u'v'} = \varepsilon \frac{\partial U}{\partial r} \quad (1)$$

C. Secondary Heading

Secondary headings should be aligned to the left and designated by A, B, C, and so on. The first letter of each word is capitalized except for prepositions, articles, and conjunctions. The font is 10 point size.

In Equation (1), U and V are the axial and radial wind speeds, respectively, x is the axial distance, r is the radial distance coordinate from the wake centerline, and $\overline{u'v'}$ is the Reynolds stress. The Reynolds stress generated by the wake is obtained by a separate equation in Equation (1) that includes the eddy viscosity ε that was obtained by an empirical equation available in literature [15].

To solve Equation (1), a boundary value of the velocity deficit is required and given by empirical equations [15].

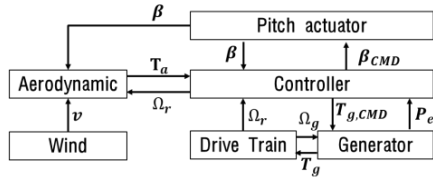


Fig. 2. Wind turbine block diagram model.

TABLE I
GENERAL INFORMATION OF NREL 5MW WIND TURBINE

Rotor diameter	126 m
Cut-in, rated, cut-out Wind speed	3m/s, 11.4m/s, 25m/s
Hub height	90 m
Rated rotor speed	12.1rpm
Rated tip speed ratio	7.08

$$D_M = \frac{U_0 - U_w}{U_0} = C_T - 0.05 - \frac{(16C_T - 0.5)I_0}{1000} \quad (2)$$

where D_M is the velocity deficit, U_0 is the undisturbed wind velocity, U_w is the wind velocity in the wake region, C_T is the thrust coefficient, and I_0 is the ambient turbulence intensity in percentage.

The eddy-viscosity model was solved by Thomas algorithm with Crank Nicolson center differencing scheme of the finite difference method, and the wind field within the wind farm was obtained.

The wakes caused by multiple upstream wind turbines in a wind farm are merged and affect downstream wind turbines. To represent the effect mathematically, the wakes were combined by the square root of the sum of the square of the deficits—a technique commonly used in commercial codes [16].

D. Wind Turbine Model

In this study, a 5MW research wind turbine designed by NREL was used as the wind turbine model because all the parameters needed to model the wind turbine are available online. Table I shows the general information of the wind turbine. Detailed information is available in literature [17].

Fig. 2 shows the block diagram of the dynamic wind turbine model implemented to the simulation tool. The wind turbine was simulated using MATLAB or Simulink. After modeling the wind turbine, the Simulink model was debugged and converted into a c-code to reduce the simulation time and be implemented in the simulation tool.

As shown in the figure above, the turbine model requires wind and power demand as inputs for simulation. It consists of an aerodynamic model, a drive train model, generator model, pitch actuator model, and a controller model. The aerodynamic model calculates the aerodynamic torque and thrust force at the rotor. The drive train model determines the rotor RPM and shaft torque. The generator model calculates the power generation. The pitch actuator and

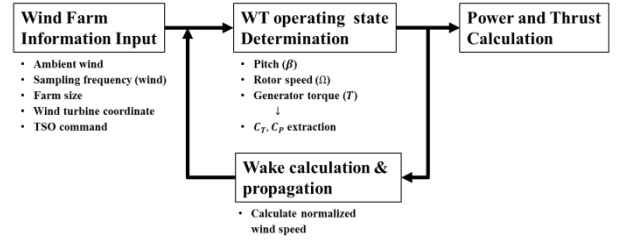


Fig. 3. Wind Farm Simulation Algorithm.

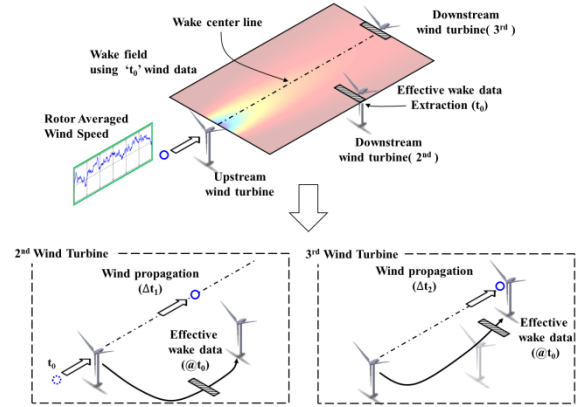


Fig. 4. Wind propagation within a wind farm.

controller simulate max-Cp and the collective pitch control for power regulation control. Overall, the wind turbine model calculates the dynamic turbine power output. More information on the wind turbine model is available in literature [17], [18].

In Fig. 2, β is the blade pitch angle, T is the torque, Ω is the rotational speed, and P_e is the electrical power. Subscripts a , r , g , and CMD are the aerodynamic, rotor, generator, and command, respectively. β_{CMD} is the blade pitch command, and $T_{g,CMD}$ is the generator pitch command.

E. Wind Farm Modeling

Fig. 3 shows the wind farm simulation algorithm with the computed values and the input and output variables associated to them. The simulation tool runs in the time-domain with inputs including ambient wind data with a sampling frequency, wind turbine coordinates, and the total power demand from the transmission system operator (TSO).

In the calculation shown in Fig. 4, the simulation tool determines the wind turbine priority based on the coordinates of the wind turbines. A high wind turbine priority implies that the wind turbine is located upstream. The wake generated from a high-priority wind turbine is applied to lower priority wind turbines to simulate the wake effect. In reality, wind turbines with relatively low priority are affected by the multiple wakes generated by high-priority wind turbines located upstream. The wake effect to downstream wind turbines can be divided into three different conditions: full wake, partial wake, and out-of-wake conditions.

As shown in Fig. 4, a small wind farm with three wind

turbines was considered. The wake field of the wind turbine located farthest upstream is calculated using the wake model. The wake field is limited to $\pm 3RD$ (RD : Rotor Diameter) laterally and up to the wind turbine located farthest downstream along the flow direction. After calculating the wake field of the wind turbine located farthest upstream, the simulation tool calculates the downstream wind turbine's relative position, and determines the wake condition. If the downstream wind turbine is within the full or partial wake region, the wake data are extracted from the pre-calculated wake field that will affect the downstream wind turbine and the averaged rotor value of the wake is applied to the downstream wind turbine after the correct time interval Δt_1 considering the propagation time. Δt_1 is the elapsed time when the wind data from the first wind turbine reaches the second wind turbine. The calculation of the elapsed time is based on frozen turbulence assumption by Taylor that the turbulence characteristic in the wind does not change, and the wind propagates with its mean wind speed and turbulence. Hence the mean wind speed was used to calculate the elapsed time. For the second and third wind turbines, the same algorithm is performed for simulation. However, as mentioned earlier, if the wind turbine priority is low, the upstream wind turbines will generate more than one wake effect. The third wind turbine in Fig. 4 will experience the wake generated from the first and second wind turbine, and the wake will be applied after the time interval Δt_2 . Δt_2 is the time duration when the wind data passes from the first wind turbine and reaches the third wind turbine. In this case, the wake is calculated using the superposition algorithm for multiple wakes mentioned earlier and the averaged rotor value is finally applied to the third wind turbine to calculate the power output.

Although the simulation tool considered wind and wake propagation in the time domain, the wake model that was used in this study is based on the Reynolds-averaged Navier-Stokes equation that is basically a static model. Hence the simulation tool calculates the steady wake field in each step according to various wind speeds to simulate turbulent wind flow in the time domain, and the result is applied to downstream wind turbines using same algorithm. A similar method known as the sliding mesh method is used in commercial CFD codes for transient flow field analysis using steady-state solutions based on Reynolds-averaged Navier-Stokes equation [19].

III. SIMULATION RESULT AND VALIDATION

A. Wake from a Single Turbine

Fig. 5(a) shows the wake field calculated in the downstream from NREL 5MW reference wind turbine using the Ainslie's eddy viscosity model. The thrust coefficient, C_T , used for the wake calculation was 0.8 that is

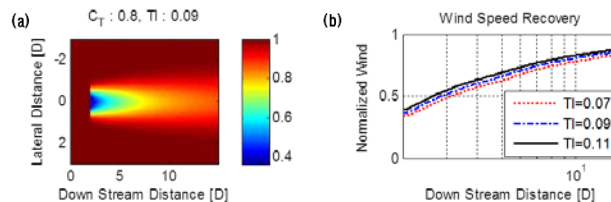


Fig. 5. Eddy viscosity wake shape (a) solved by Thomas algorithm and wind speed recovery with turbulence intensity increasing (b).

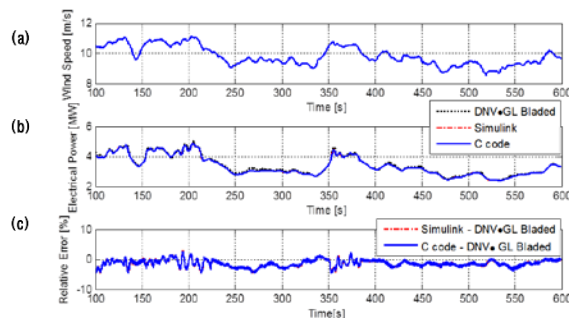


Fig. 6. Electrical power outputs for the turbulent wind data obtained from the developed tools and DNV-GL Bladed for (a) wind speed, (b) electrical power, and (c) relative error.

approximately the thrust coefficient that modern wind turbines have in operations below their rated wind speeds. As shown in the figure, the solution is obtained from the two-rotor diameter downstream from the wind turbine, and the axi-symmetric wind field is expanded in the lateral direction.

The wind speed at two-rotor diameter downstream was approximately five or six m/s and increased to approximately 8 or 9 m/s at a ten-rotor diameter downstream. With a higher ambient turbulence intensity, the recovery of wind speed in the wake region becomes faster as shown in Fig. 5(b).

B. Validation of Wind Turbine Power Output

To validate the wind turbine model used in the wind farm simulation program, the result obtained from the wind turbine model was compared with the commercial wind turbine design and certification program, DNV-GL bladed.

Fig. 6(b) shows the comparison of the power output from the wind turbine model (based on Simulink and c code) and the result obtained from DNV-GL bladed in the time domain. For a simulation, the wind turbine model requires the average hub-height wind speed, however, DNV-GL bladed uses a three-dimensional wind field. The average rotor wind data obtained from DNV-GL bladed that is the averaged data of the three-dimensional wind field over the rotor was used for the wind turbine model. The average rotor wind data used for the simulation is shown in Fig. 6(a). As shown in Fig. 6 (b), the electrical power output from the wind turbine model is very close to the power output calculated from DNV-GL bladed. The maximum relative error is lower than 5%, as

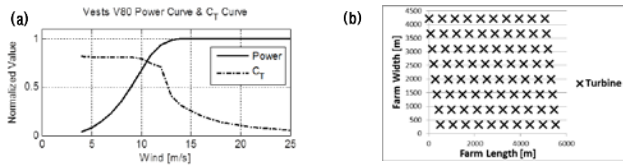


Fig. 7. The Power Curve and C_T for Vestas V80 2MW (a) and Horns Rev1 offshore wind farm layout.

shown Fig. 6(c).

Therefore, the wind turbine model used for the wind farm simulation in this study was found to be valid.

C. Validation of Power Output from a Wind Farm

To simulate and validate the wake field in a wind farm, the Horns Rev 1 offshore wind farm in Denmark was considered because the power output from the wind farm is available in literature.

The Horns Rev 1 consists of 80 Vestas V80 2 MW wind turbines with 8 rows and 10 columns. The turbine spacing is seven times the rotor diameter of the turbines. In literature, the power output from the wind farm at a wind length speed of 10 m/s is given for different wind directions with an interval of 5° . For the simulation, the dynamic model of the wind turbine and a suitable wind turbine controller are required. However, obtaining such data or model of commercial wind turbines such as V 80 from the wind turbine manufacturer is not possible. Hence the wind turbine's power and thrust curves as a function of wind speed were used to simulate Horns Rev 1 offshore wind farm just for validation instead of using the dynamic wind turbine model and the controller. The wind data consisting of 500 sets with a constant wind speed of 10 m/s were used for this simulation. The power curve and thrust curve of the turbine were obtained from WindPRO, a commercial code used to predict annual power productions of wind farms. The curves and the layout of Horns Rev 1 wind farm are shown in Fig. 7.

Fig. 8 shows the simulation results for the wind farm and the experimental results available in literature. The total simulation time was approximately 10 seconds. The y axis represents the power summed for each column of wind turbines divided by the power summed for the first column of wind turbines. The x-axis represents the distance by multiplying the rotor diameter. For the comparison with the experimental data, the simulation was performed for different wind directions from -15° to $+15^\circ$ with an interval of 5° . Simulation was performed by fixing the wind direction with varying the base angles of the wind farm layout.

As shown in Fig. 8, the power output drops dramatically in the second column compared to the first column and gradually drops in the subsequent columns. The results from the simulation tool mostly do not fully predict actual power output when the wind direction is close to 0° . This implies that the eddy viscosity wake model used in the simulation overestimated the velocity deficit in the wake

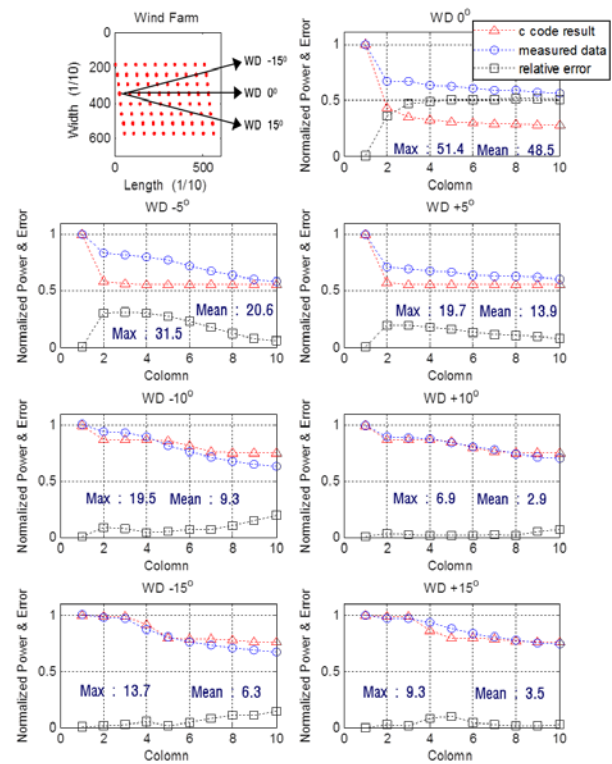


Fig. 8. Simulation result of Horns Rev 1 wind farm.

field. The largest discrepancy occurred when the wind direction is $WD 0^\circ$. When the wind direction changes from $WD 0^\circ$ to $WD \pm 15^\circ$ the discrepancy appears to decrease. The change of discrepancy with wind direction is attributed to meandering, a fluctuation of the wake center. In reality, the wake center deviates from the straight downstream direction, and the downstream wind turbine might be partially affected by the wake generated by the upstream wind turbine because of meandering. However, this is not considered in the eddy viscosity wake model.

D. Dynamic Simulation of Wind Farm

Figure 9 shows the dynamic simulation results from the simulation tool. The same Horns Rev wind farm layout in the previous section was also used. For the dynamic simulation, 5MW research wind turbine models developed by NREL were used instead of Vestas 2MW wind turbines because all the turbine information needed is available in literature. The mean wind speed was 10 m/s and the turbulence intensity was 9%. The wind direction was $WD 0^\circ$. The time interval of the simulation was one second. It took approximately 80 seconds to simulate 80 wind turbines for 2200 seconds.

Based on the figure above, wind speed U of the first wind turbine is significantly higher than those of wind turbines 28 and 80. Pitch angle β of the first wind turbine is changed when the wind speed exceeds the rated wind speed because of the high wind speed. For the other two wind turbines, the pitch angle remains at the fine pitch because of low wind

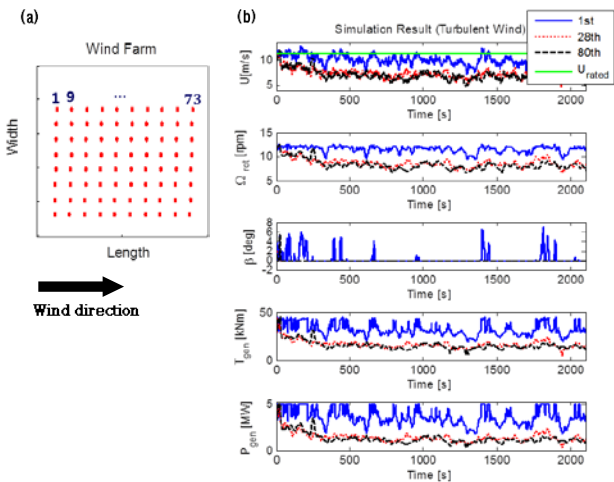


Fig. 9. Dynamic Simulation Results of Horns Rev Wind Farm. (a) Wind Farm Layout, (b) Dynamic Simulation Results. U : wind speed, Ω_{rot} : rotational speed of rotor, β : pitch angle, T_{gen} : generator torque, P_{gen} : power generation.

speed. As wind speed varies, the rotational speed of the rotor, Ω_{rotor} , changes, and the generator torque, T_{gen} , is changed for max- C_p control. Power generation, P_{gen} , varies although the rated power is not exceeded. The power generation of wind turbine 80 is significantly lower than that of wind turbine 1 but is slightly lower than that of wind turbine 28. This is similar to the result in Section C.

IV. CONCLUSION

In this study, a time-domain fast-simulation tool to predict the power outputs from wind turbines in an offshore wind farm using C code was constructed. The simulation tool calculates two-dimensional wake fields in a wind farm to obtain the wind speed for individual wind turbines and computes power outputs from wind turbines based on the wind speeds and proper control mechanism. The developed tool calculated power outputs from a Danish wind farm and the results were compared with the experimental results available in literature. The eddy-viscosity wake model in the simulation tool overestimated the wake field and finally did not fully predict the electrical power, particularly when the wind turbines are in line with the wind direction. Discrepancy occurred because the eddy viscosity model did not consider the meandering effect. The developed tool successfully calculated the dynamic power outputs from the NREL 5MW wind turbines in Horns Rev 1 wind farm with wind turbines, as well as the wind speed variations, and the wind turbine states including pitch angle, rotational speed of the rotor, generator torque, and power generation.

ACKNOWLEDGMENT

This work was supported by the Human Resources

Development program (No. 20134030200240) of the Korea Institute of Energy Technology Evaluation and Planning (KETEP) grant funded by the Korea government Ministry of Trade, Industry, and Energy. The present work is also a result of the project “Development of the design technologies for a 10MW class wave and offshore wind hybrid power generation system and establishment of the sea test infrastructure” granted by the Ministry of Oceans and Fisheries. All support is gratefully acknowledged.

This paper has been presented to World Wind Energy Conference 2014 and International Conference on Wind energy Grid-Adaptive Technologies 2014.

REFERENCES

- [1] R. A. Rivas, J. Clausen, K. S. Hansen, and L. E. Jensen, “Solving the turbine positioning problem for large offshore wind farms by simulated annealing,” *Wind Energy*, Vol. 33, No. 3, pp. 287-297, 2009.
- [2] S. Şişbot, Ö. Turgut, M. Tunç and Ü. Çamdalı, “Optimal positioning of wind turbines on gökçeada using multi-objective genetic algorithm,” *Wind Energy*, Vol. 13, No. 4, pp. 297-306, 2010.
- [3] A. Kusiak and Z. Song, “Design of wind farm layout for maximum wind energy capture,” *Renewable Energy*, Vol. 35, No. 3, pp. 685-694, Mar. 2010.
- [4] L. Rademakers, H. Braam, T. Obdam and R. vd Pieterman, “Operation and maintenance cost estimator (OMCE) to estimate the future O&M costs of offshore wind farms,” in *Proc. European Offshore Wind 2009 Conference, Stockholm, Sweden*, pp. 14-16, 2009.
- [5] G. Corten and P. Schaak, “Heat and flux,” *Patent Number WO2004111446*, 2003.
- [6] B. Arno, B. Edwin, K. Stoyan, S. Feike, and Ö. Hüseyin, “Wind farm design and active wake control,” *Europe's Premier Wind Energy Event*, 2014.
- [7] E. Bot, G. Corten, and P. Schaak, “A program to determine energy yield of wind turbines in a wind farm,” 2011.
- [8] P. Eecen and E. Bot, “Improvements to the ECN wind farm optimisation software ‘FarmFlow’,” *the European Wind Energy Conference & Exhibition*, 2010.
- [9] J. Pierik, U. Axelsson, E. Eriksson and D. Salomonsson, *EeFarm II. Description, Testing and Application*, Energy Research Centre of the Netherlands, 2009.
- [10] P. E. Réthoré, P. Fuglsang, T. J. Larsen, T. Buhl, and G. C. Larsen, “TOPFARM wind farm optimization tool,” Risø National Laboratory for Sustainable Energy, Technical University of Denmark, 2011.
- [11] P. Fleming, P. Gebraad, J. van Wingerden, S. Lee, M. Churchfield, A. Scholbrock, J. Michalakes, K. Johnson and P. Moriarty, “The SOWFA super-controller: A high-fidelity tool for evaluating wind plant control approaches,” in *Proc. EWEA Annual Meeting, Vienna, Austria*, 2013..
- [12] J. D. Grunnet, M. Soltani, T. Knudsen, M. N. Kragelund, and T. Bak, “Aeolus toolbox for dynamics wind farm model, simulation and control,” in *The European Wind Energy Conference & Exhibition, EWEC*, 2010.
- [13] T. von Karman, “Progress in the statistical theory of turbulence,” in *Proc. Natl.Acad.Sci.U.S.A.*, Vol. 34, No. 11,

pp. 530-539, Nov. 1948.

- [14] International Electrotechnical Committee, "IEC 61400-1: Wind Turbines part 1: Design requirements," International Electrotechnical Commission, 2005.
- [15] J. F. Ainslie, "Calculating the flowfield in the wake of wind turbines," *J. Wind Eng. Ind. Aerodyn.*, Vol. 27, No. 1-3, pp. 213-224, Jan. 1988.
- [16] I. Katic, J. Højstrup, and N. Jensen, "A simple model for cluster efficiency," in *European Wind Energy Association Conference and Exhibition*, pp. 407-410, 1986.
- [17] J. M. Jonkman, S. Butterfield, W. Musial, and G. Scott, *Definition of a 5-MW reference wind turbine for offshore system development*, National Renewable Energy Laboratory Golden, CO. 2009.
- [18] K. Kim, C. Lim, Y. Oh, I. Kwon, N. Yoo, and I. Paek, "Time-domain dynamic simulation of a wind turbine including yaw motion for power prediction," *International Journal of Precision Engineering and Manufacturing*, Vol. 15, No. 10, pp. 2199-2203, Oct. 2014.
- [19] A. Fluent, "Ansys Fluent Theory Guide," ANSYS Inc., USA. 2011.



Hyungyu Kim received his M.S. degree in Mechanical and Mechatronics Engineering from Kangwon National University, Chuncheon, Republic of Korea in 2014. His research interests include wind turbine wakes, wind farm simulation, and wind farm control.



Kwansoo Kim received his M.S. degree in Mechanical and Mechatronics Engineering from Kangwon National University, Chuncheon, Republic of Korea in 2014. His research interests include wind turbine simulation and control.



Insu Paek received his B.S. in Mechatronics Engineering from Kangwon National University, Chuncheon, Republic of Korea in 1997, and his M.S. in Mechanical Engineering from the University of Texas at Austin, USA, in 2000. He received his Ph.D. in Mechanical Engineering from Purdue University, Indiana, USA, in 2005. He worked as a Postdoctoral Researcher at Purdue University and McGill University in 2006 and 2007. He is currently an Associate Professor in Mechatronics Engineering, Kangwon National University. His research interests are various topics of wind energy including wind turbine and farm simulation and control, wind resource assessment and wind farm design, and power performance testing of small wind turbines.



Neungsoo Yoo received his B.S. and M.S. in Mechanical Engineering from Yonsei University and his Ph.D degree in Aeronautic and Mechanical Engineering from ENSMA of Poitiers University in 1982. His research interests include wind turbine aerodynamics, wind farm micro-siting, wind resource assessment, and power performance testing of wind turbines.